# Digital Pre-Compensation of Doppler Frequency Shift in Coherent Optical Satellite Communications

Sylvain Almonacil[(1)†], Rajiv Boddeda[(1)], Tituan Allain[(1)], Daniel Romero Arrieta[(1,2)] and Sébastien Bigo[(1)]

[(1)]Nokia Bell Labs, Route de Villejust, 91620 Nozay, France †sylvain.almonacil@nokia-bell-labs.com
[(2)]University Paris-Saclay, Route de l'Orme aux Merisiers – RD128, 91190 Saint-Aubin, France

***Abstract*** *We propose to compensate the Doppler shift in satellite communications digitally by combining digital pre-emphasis and clipping. Without laser wavelength tuning, we achieve up to 10 GHz compensation at 500 Gbps line rate with less than 0.7 dB additional optical launched power.*

## Introduction

Satellite communications have caught growing interest to bring broadband services in low-density populated areas or to complement terrestrial networks with temporary connectivity in disaster zones. To perform such communications, free space optical links are promising alternatives to radio links because they can provide ≈ 1000x larger bandwidth while saving > 50% in size, weight and power consumption[1,2]. While state of the art free space optical links carry 10G data[3], digital coherent optics would bring a capacity breakthrough with ≥100G per coherent space terminal.

However, free space optical links suffer from propagation impairments unknown in terrestrial fibre systems[1]. For instance, systems based on moving satellites undergo a Doppler shift due to the relative motion between the transmitter (Tx) and the receiver (Rx). From Kepler's law, it can be shown that the speed of satellites increases as their altitude decreases. Hence a free space optical link established to/from a low Earth orbit satellite (typical altitude <2000 km) experiences a significant Doppler shift up to several GHz[1,4]. At an altitude of 400 km, the worst-case Doppler shift can reach up to ±10 GHz for satellites moving in opposite directions. Doppler effect can be understood with Fig.1, considering two low Earth orbit satellites moving in opposite directions. If the Tx of satellite n°1 is set at frequency $\nu_1$, then the frequency seen at the Rx of satellite n°2 is $\nu_1 + \Delta\nu$, with $\Delta\nu > 0$ being the Doppler shift. Conversely, if the Tx frequency of satellite n°2 is set at $\nu_2$, then the frequency seen by the Rx of satellite n°1 is $\nu_2 + \Delta\nu$. With coherent technology, the Doppler shift results in a time-varying mismatch $\Delta\nu$ between the Tx laser and the Rx local oscillator frequencies. Thus, the fast pointing and acquisition between two satellite terminals should come with an equally time-dependent tuning of the frequency offset between the Tx and Rx lasers. In practice, several solutions can be worked out. For instance, the wavelength of laser sources[1] can be tuned in pre-(at Tx) or post-(at Rx) compensation mode[4], as per radio[5], but this requires a command and control circuitry which increase the Tx/Rx cost and complexity

Alternatively, we propose to compensate for the Doppler shift without using tunable lasers with a new block in the Tx digital signal processing chain (pre-compensation). This block shifts the signal digitally in the frequency domain by the opposite of the Doppler shift value. When received, the signal is therefore aligned with the Rx local oscillator frequency. Note that the digital compensation of the Doppler effect could also be performed in the receiver[6] but the typical brick-wall filter shape of analog-to-digital converters[7] can make it prohibitively difficult to recover the high frequencies of the shifted signal. The paper is organized as follows: first, we discuss the implementation of Digital Doppler Shift Compensation (DDSC) and second, we assess its performance experimentally.

## Principle of the Digital DS Compensation

The DDSC is a Tx-DSP block which multiplies the complex signal by $e^{2i\cdot\pi\cdot\Delta\nu\cdot t}$, with $t$ the discrete time defined by the Tx sampling frequency and $\Delta\nu$ the Doppler shift. It can be inserted before the digital compensation of the frequency response (digital pre-emphasis, DPE). The DDSC results in an asymmetrical spectrum, as shown in Fig. 2a (dashed line). The maximum shift that DDSC can compensate depends on the digital-to-analog converter (DAC) sampling frequency $f_s$ and on the signal spectrum. With root-raised-cosine signal spectra, the maximum absolute frequency component is $R\cdot(1+\beta)\cdot 0.5$, with $R$ the symbol rate and $\beta$ the rolloff factor. It must not exceed

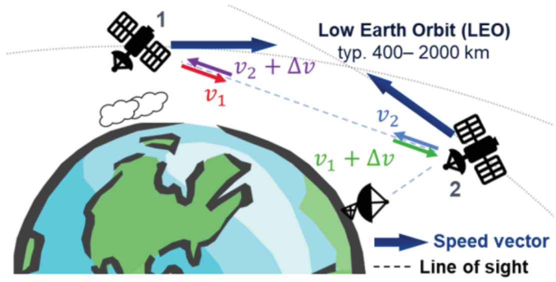


**Fig. 1:** Typical low Earth Orbit scenario. When the line of sight is parallel to the speed vector, the Doppler effect is maximal and since the satellites are moving towards each other, both of them will see a relative shift towards higher frequencies.

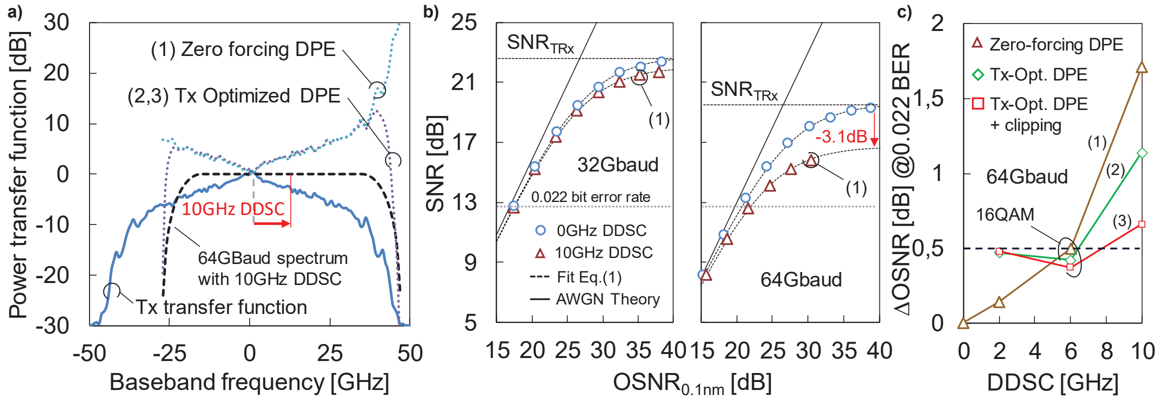


**Fig. 2:** a) Frequency responses of the Tx; the 64 Gbaud signal (root-raised-cosine rolloff 0.2) with 10 GHz Digital Doppler Shift Compensation (DDSC); the digital pre-emphasis (DPE) filters for scenarios (1) zero-forcing DPE, (2) Tx-optimized DPE and (3) Tx-optimized DPE and clipping. b) Signal-to-noise ratio versus optical signal-to-noise ratio for 32 and 64 Gbaud/16QAM without DDSC and with 10 GHz DDSC and scenario (1). c) Optical signal to noise ratio penalty for the three scenarios.

the DAC Nyquist frequency $f_s/2$ to avoid aliasing. For instance, with 64 Gbaud and $\beta = 0.2$, the minimum $f_s$ for 10 GHz DDSC is ~97 GS/s. Here, we use a 100 GS/s DAC for our experiments. In the following, we assume that the Doppler shift is known at every moment by the prediction of the satellite motion in the sky by precomputed ephemerides[8], possibly provided from the ground by control channels.

## System Performance Analysis

To assess the effect of our digital DDSC on a typical coherent system, we connected a Tx and an Rx in back-to-back. The Tx spectral transfer function is provided in Fig. 2a. It exhibits a -10 dB bandwidth of ~35 GHz. We superimposed to this response the two DPE spectral transfer functions that we implemented (all shown at 10 GHz DDSC, dotted lines). They correspond to 2 DPE scenarios: (1) a zero-forcing DPE (inversing the Tx transfer function at all frequencies); (2) a Tx-optimized (Tx opt.) DPE[9] for which we use an effective resolution of 4 bits, extracted from our previous work over the same equipment[10], and reduced by 1 bit to account for the entire Tx chain. We extended the second scenario with a third one (3) where we clip the waveforms loaded into the DAC memory. Although clipping is known for minimizing the DAC distortions[11,12], we use it for its strong impact on the Tx output power.

A variable optical attenuator and an Erbium-doped fiber amplifier are used for noise loading. At the Rx, we employ a 200 GS/s real-time oscilloscope with >70 GHz electrical bandwidth. The traces are processed off-line by resampling at 2 samples per symbol, constant modulus equalization, carrier and phase recovery, down sampling at 1 sample per symbol and symbol decision. To emulate the Doppler shift and its compensation, the local oscillator frequency is shifted by the same amount as the DDSC.

We assess the system performance by measuring the electrical signal-to-noise ratio (SNR) versus the optical SNR (OSNR) normalized to 0.1nm and report the results in Fig. 2b with 16QAM data at 32 Gbaud and 64 Gbaud. In absence of DDSC, the SNR grows with OSNR until it saturates, which can be described by the well-known equation:

$$SNR = (1/SNR_{TRx} + 1/\xi OSNR)^{-1} \qquad (1)$$

where $SNR_{TRx}$ is the Tx-Rx induced distortions and ξ the conversion factor from the OSNR measurement bandwidth. With DDSC, SNR is found to saturate faster with OSNR, which suggests that $SNR_{TRx}$ has been impaired. Measurements at 64 Gbaud indicate even faster saturation than at 32 Gbaud. We fitted them with Eq.(1) to extract the $SNR_{TRx}$ = f(OSNR→∞). At 32 Gbaud, the impact of DDSC is relatively small i.e. a reduction of 0.9 dB of $SNR_{TRx}$ while it reaches 3.1 dB at 64 Gbaud. This is the result of the attenuation of the high frequencies of the signal due to the limited Tx bandwidth, especially from the DAC but also the driver amplifier and the Mach-Zehnder modulator. These impairments are enhanced with DDSC because the DPE strongly amplifies the frequencies of the signal in the leftmost and rightmost parts of the Tx transfer function (Fig. 2a). This increases the signal peak-to-average power ratio and hence the distortions due to the limited DAC effective resolution.

The corresponding OSNR penalties (ΔOSNR) targeting 0.022 bit error rate without encoding are shown in Fig. 2c. For 16QAM at 64 Gbaud, they reach a maximum value of 1.7 dB for DPE scenario (1) and go down to 1.1 dB and 0.7 dB for scenarios (2) and (3), respectively. The improvement originates from the fact that Tx opt. DPE minimizes the DAC output mean square error at the selected effective resolution. However, for 6 GHz DDSC, the Tx-optimized DPE gives a similar performance as the zero-forcing DPE because below ~35 GHz the DPE transfer functions are almost identical. With DPE

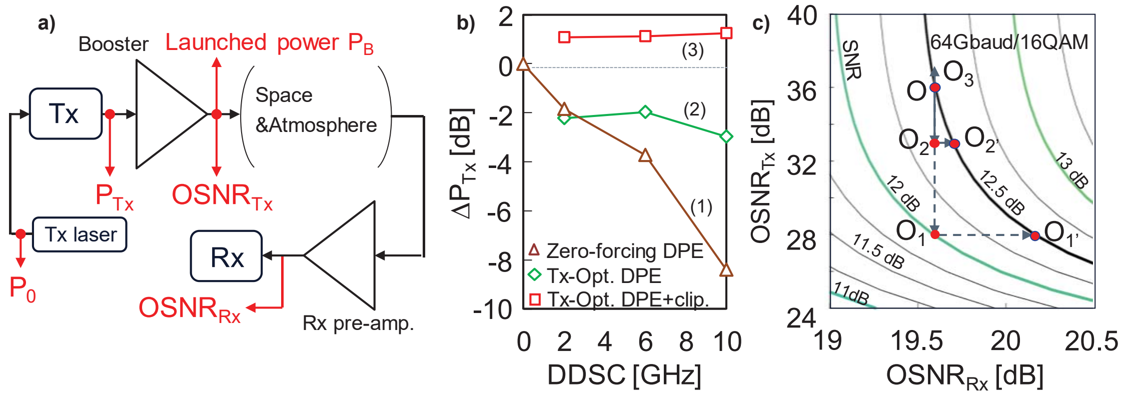


**Fig. 3:** a) Considered satellite system. b) Measured transmitter output power $\Delta P_{Tx}$ variation with DDSC for the three investigated scenarios: (1) Zero-forcing DPE; (2) Tx-optimized DPE and (3) Tx-optimized DPE with clipping. c) System SNR abacus for 64 Gbaud/16QAM versus booster output optical signal to noise ratio ($OSNR_{Tx}$) and receiver pre-amplifier $OSNR_{Rx}$.

scenario (3), we obtain further performance gain by slightly clipping the waveform. One important condition to benefit from clipping is that signal-to-clipping noise ratio must remain much higher than $SNR_{TRx}$. Here, we keep it >35 dB. However, should clipping be used with zero-forcing DPE (scenario 1) to mitigate DDSC impairments, we computed 14 dB signal-to-clipping noise ratio, which would deteriorate the system performance.

If Fig.2c, we also observe for DPE scenarios (2) and (3) a slight degradation with respect to scenario (1) for DDSC<6 GHz. This could be attributed to the frequency dependence of the effective resolution, which we neglected here. The effective resolution parameter was computed for 10 GHz DDSC and is under-optimized for DDSC at smaller frequency shifts.

We now extend the evaluation of the performance to the full satellite system depicted in Fig. 3a, for which two optical amplifiers at Tx and Rx are interfaced with two telescopes and produce most of the system noise. We particularly address on another impairment caused by DDSC, namely the relative reduction $\Delta P_{Tx}$ of Tx output power $P_{Tx}$. This reduction translates into a reduction of OSNR at the output of the high-power amplifier booster ($OSNR_{Tx}$). We report in Fig. 3b the measured $\Delta P_{Tx}$ variation for 64 Gbaud/16QAM caused by DDSC in the three DPE scenarios. For scenario (1), $\Delta P_{Tx}$ can be as high as -8 dB at 10 GHz DDSC while it reduces to less than -3dB in (2) and can even slightly increase in (3).

Without clipping, the loss on power by $\Delta P_{Tx}$ translates into a second OSNR penalty, which adds to the first $\Delta$OSNR penalty due to the $SNR_{TRx}$ variations. Insight can be provided by segmenting the booster and the Rx optical preamplifier contributions from Eq.(1):

$$SNR = (1/SNR_{TRx}+1/\xi OSNR_{Tx} +1/\xi OSNR_{Rx})^{-1} \quad (2)$$

In Fig. 3c, we discuss system trade-offs with iso-SNR abacus for various ($OSNR_{Tx}$, $OSNR_{Rx}$) values, while neglecting $1/SNR_{TRx}$. We take the example of 16QAM modulation which would require SNR of 12.5 at 0.022 bit error rate without encoding (black solid line). The design operating point O in Fig. 3c is obtained by considering $OSNR_{Tx}$~36 dB and assuming that without DDSC the system operates at 12.5 dB SNR. For scenario (1), DDSC induces a decrease in Tx output power by $\Delta P_{Tx}$ = -8 dB which translates into a decrease of $OSNR_{Tx}$ by the same amount. This is represented by the transformation $OO_1$ (vertical translation) in Fig. 3c. In these conditions the SNR is found to be reduced by 0.5 dB penalty (change of iso-SNR line) which can be mitigated by raising the launched power $P_B$, and hence $OSNR_{Rx}$, by +0.6 dB (transformation $O_1O_{1'}$, horizontal translation). Another solution would be to increase the Tx laser power $P_0$ by +8 dB, which is generally challenging. With scenarios (2), the variation $\Delta P_{Tx}$ shrinks to -3 dB (transformation $OO_2$), which can be mitigated by increasing the launched power by +0.15 dB (transformation $O_2O_{2'}$). Thus, to mitigate all DDSC penalties (accounting for $\Delta$OSNR from Fig 2c and $\Delta P_{Tx}$ induced penalties) in scenarios (1) and (2), the booster should deliver 1.7+0.6=2.3 dB and 1.1+0.15=1.25 dB extra power, respectively.

With clipping, i.e. scenario (3), the point O is slightly moved up vertically (transformation $OO_3$). Therefore, clipping recovers almost all the $\Delta P_{Tx}$ induced penalty. In that case the total OSNR penalty left to mitigate is just $\Delta$OSNR = 0.7 dB which can be mitigated by adding the same amount to the optical launch power.

## Conclusion

We propose a digital pre-compensation of the Doppler shift in satellite communications without using tunable lasers. For 64 Gbaud/16QAM, by carefully compensating the bandwidth limitation of the digital-to-analog converter and by slightly clipping the generated signal, we mitigate up to 10 GHz Doppler shift with no more than 0.7 dB of additional optical launched power.

## References


[1] Kaushal H. and Kaddoum G., "Optical Communication in Space: Challenges and Mitigation Technique," in IEEE Communications Surveys and Tutorials, 2017, 19, 1, pp. 57-96, DOI: 10.1109/COMST.2016.2603518.

[2] Estarán J. M., Pointurier Y. and Bigo S., "FSO SpaceComm Links and Its Integration with Ground 5G Networks," in Proc. of Optical Fiber Conf. San Diego, USA, 2020, paper M4F.1.

[3] TeSat press release, "ISS Preparing for Gigabit Era," Aug. 10th 2020, avalaible online: https://www.tesat.de/news/blog/information/83-news/880-iss-preparing-for-gigabit-era.

[4] Ando T., Haraguchi E., Tajima K. et al., "Homodyne BPSK receiver with Doppler shift compensation for inter satellite optical communication," in Proc. of International Conf. on Space Optical Systems and Applications, Santa Monica, USA, 2011, DOI: 10.1109/ICSOS.2011.5783683.

[5] Cao Y. and T. Zhang, "Two stage frequency offset pre-compensation scheme for satellite mobile terminals," in Proc. of 13th Conf. on Industrial Electronics and Applications (ICIEA), Wuhan, China, 2018, DOI: 10.1109/ICIEA.2018.8397700.

[6] Rosenkranz W. and Schaefer S., "Receiver Design for Optical Inter-Satellite Links Based on Digital Signal Processing," in Proc. of 18th International Conference On Transparent Optical Networks (ICTON), Trento, Italy, 2016, paper Tu.B2.2, DOI: 10.1109/ICTON.2016.7550381.

[7] Hu Q., Schuh K., Chagnon M. et al., "Up to 94 GBd THP PAM-4 Transmission with 33 GHz Bandwidth Limitation," in Proc of 44th European Conf. On Optical Communication, Roma, Italy, 2018, paper Th3F.6, DOI: 10.1109/ECOC.2018.8535334

[8] Wu B. and Xu Y., "Doppler Shift Estimation Using Broadcast Ephemeris in Satellite Optical Communication," in Proc. of 25th Wireless and Optical Communication Conference (WOCC), Chengdu, China, 2016, DOI: 10.1109/WOCC.2016.7506577.

[9] Napoli A., Mezghanni M. M., Rahman T. *et al.*, "Digital Compensation of Bandwidth Limitations for High-Speed DACs and ADCs," in Journal of Lightwave Technology, 2016, 34, 13, pp. 3053-3064, DOI: 10.1109/JLT.2016.2535487.

[10] Almonacil S., Jennevé P., Ramantanis P. et al., "DAC Jitter Requirements for High-Speed Optical Networks,' in Proc of 44th European Conf. On Optical Communication, Roma, Italy, 2018, paper Th1D.4, DOI: 10.1109/ECOC.2018.8535567.

[11] Almonacil S., Boitier F. and Layec P., "Performance Model and Design Rules for Optical Systems Employing Low-Resolution DAC/ADC," in Journal of Lightwave Technology, 2020, 38, 11, pp. 3007-3014. DOI: 10.1109/JLT.2020.2984924.

[12] V. D. Hout M., V. D. Heide S. and Okonkwo C., "Digital Resolution Enhancer Employing Clipping for High-Speed Optical Transmission," in Journal of Lightwave Technology, 2020, 38, 11, pp. 2897-2904. DOI: 10.1109/JLT.2020.2988377.